

# Validation of Sediment Transport Model Using Hydraulic Experiment Data to Assess the Influence of Grain Size and Reflection Wave on Tsunami Deposit

津波堆積物の粒径や反射波の影響に関する  
水理実験データを用いた土砂移動モデルの検証

関西大学 社会安全研究科

山本阿子

Graduate School of Societal Safety  
Sciences, Kansai University

Ako YAMAMOTO

関西大学 社会安全研究科

高橋智幸

Graduate School of Societal Safety  
Sciences, Kansai University

Tomoyuki TAKAHASHI

静岡大学 防災総合センター

原田賢治

Center for Integrated Research and Education  
of Natural Hazards, Shizuoka University

Kenji HARADA

日本工営株式会社

櫻庭雅明

NIPPON KOEI Co., Ltd.

Masaaki SAKURABA

日本工営株式会社

野島和也

NIPPON KOEI Co., Ltd.

Kazuya NOJIMA

## SUMMARY

To improve tsunami prediction, it is important to consider paleo tsunami records. Tsunami deposits can provide many paleo tsunami records; however, the formation mechanism of tsunami deposits remains unclear. Furthermore, numerical analysis focusing on tsunami sediment in the inundation area has fewer verification examples. Therefore, in this study, we conducted hydraulic experiments to elucidate the formation mechanism of tsunami deposits. The hydraulic experiments considered the influence of grain size and reflection wave. In addition, we investigated the characteristics of sand deposits depending on sand composition and topography (i.e., natural embankment). It was confirmed that the amount of sand deposit decreased toward the top of the run-up area. However, for the case of mixed sand which has several grain sizes, it was found that the mixing ratio influenced the composition ratio of the sand deposit in the middle of the slope area. For the case of the reflection wall, it was observed that characteristic sand deposits were formed by the return flow. We evaluated existing sand transport models using the obtained data. The results of the numerical experiments confirmed the high reproducibility of the existing models for the case with the return flow (i.e., with a reflection wall). However, for the case without return flow (without a reflection wall), it was clear that reproducibility was affected by grain size. Furthermore, it was

confirmed that the amount of sand deposit was overestimated near the top of the run-up area. Thus, we considered some problems of overcome this model.

### Key words

Tsunami deposit, uniform sand, mixed sand, bore wave, reflection wall

## 1. Introduction

Underestimation of the magnitude of tsunamis could result in their occurrence causing greater damage than might otherwise be expected. Examination of the records of many paleo tsunamis is necessary to mitigate or prevent tsunami-related damage. However, huge tsunamis such as the 2011 Tohoku tsunami occur infrequently, and there is a limit to the accuracy of estimations of tsunami scale based on historical records such as documents and stone monuments. Coastal tsunami sediments that contain records of many paleo tsunamis have been investigated using advanced coring and analytical techniques to estimate their frequency of occurrence and relative scales<sup>[1, 2]</sup>. However, quantitative estimations of scale have not been undertaken previously because the formation mechanism of tsunami deposits remains unclear. Considerable quantities of data were collected to follow the 2011 Tohoku tsunami, e.g., video, observations, measurements of the distribution and structure of the sand deposits in inundation areas. Based on field research of the deposits of the 2011 Tohoku tsunami, Abe et al.<sup>[3]</sup> reported detailed data on sediment grain size, volume, and distance from the shoreline.

One method used for the analysis of sand deposits is numerical simulation of sediment

transport by tsunamis. Takahashi et al.<sup>[4]</sup> proposed a sediment transport model (hereafter, the 2000 model), which can be applied even under nonequilibrium conditions of suspended sediment concentration, as found in a tsunami, because the suspended load and the bed load are handled separately. Suspended load is sand which transport as suspending. Bed load is sand which transport on the bottom. This model was applied using the data of the 1960 Chilean tsunami in Kesennuma. However, it was found to underestimate the amount of sand transportation under the conditions of the local topography. This model has since been improved; however, its application to the data of the 2011 Tohoku tsunami still resulted in underestimation of the amount of sand transported<sup>[5]</sup>. Takahashi et al.<sup>[6]</sup> proposed an improved model (hereafter, the 2011 model), that focused on the coefficients of the bed load and the suspended load in the equation of motion in the 2000 model. In this model, the coefficient for different grain sizes was derived by hydraulic experimentation; however, verification using other grain sizes and mixed sand compositions has not been conducted. It is necessary to collect tsunami source data for more accurate estimation of tsunami magnitude. However, techniques for the estimation of a tsunami source based on the inverse analysis of a tsunami deposit have yet

to be developed. Furthermore, many existing models have targeted the ocean area with little verification of such models in run-up areas. In addition, Jaffe et al.<sup>[7]</sup> revealed the problems associated with forward analysis and inverse analysis in the simulation of sediment transport by tsunamis. To resolve the problems, they demonstrated the need for additional quantitative data from research and experiment. Estimation of a tsunami source based on sediment deposits requires definition of the relationship between sand grain size and the flow velocity and water level of the tsunami. Both Hasegawa et al.<sup>[8]</sup> and Harada et al.<sup>[9, 10]</sup> have conducted hydraulic experiments on sediment transport and the formation of deposits in the run-up areas of tsunamis. Their work elucidated that the characteristic structure of the deposits is affected by grain size and the magnitude of the exerting force. However, the effects of mixed sand composition, topography, and structures have not been considered. Yamamoto et al.<sup>[11]</sup>

conducted hydraulic experiments using three types of mixed sand and three grain sizes of uniform sand. In their hydraulic experiments, not only were the effects of grain size and the conditions of the exerting force examined, but also structures like reflection walls were installed to change the flow conditions. Their findings revealed the deposits formed unique structures depending on the flow conditions. In this study, we reproduce the result of Yamamoto et al.<sup>[11]</sup> by the model of Takahashi et al.<sup>[4, 6]</sup>, elucidate the problems, and suggest improvements for the model.

## 2. HYDRAULIC EXPERIMENT

### 2.1 Methods and Conditions

We conducted hydraulic experiments under conditions of fixed and movable beds using a two-dimensional water channel. A part of result is Yamamoto et al.<sup>[11]</sup> shown in this experiment. The fixed bed condition was used to investigate the relation between flow condition and the wave condition. The movable

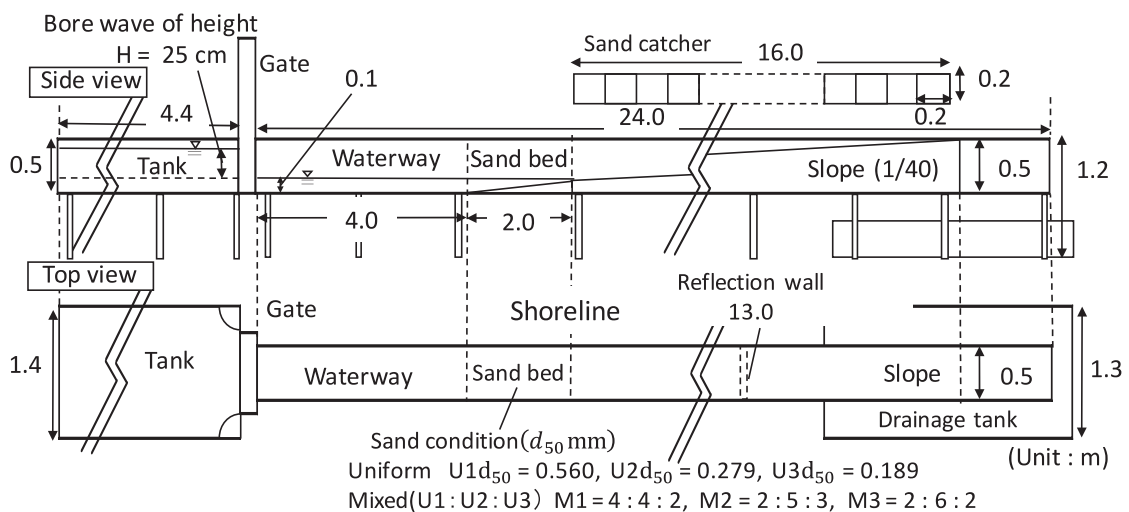


Figure 1. Experimental setup

bed condition was used to investigate the relation between the amount of sand deposit and the wave condition. Schematics of the experiments and sand conditions are shown in **Figure 1**.

As the similarity laws, Shields number and ratio of bed load rate to suspended load rate were applied. Shield number is a dimensionless version of tractive force by grain size and density. Takahashi et al.<sup>[12]</sup> studied shear stress on the sea bed in Kesenuma bay by the 1960 Chilean Tsunami. The shields number converted from the shear stress varied very frequently, and one order of a magnitude was dominant. Further, Hasegawa et al.<sup>[13]</sup> showed that the shields number have to exceed 1.0 in the tsunami sediment transport experiment. This experiment set a target of exceeding one, and 4.0 was obtained. The latter similarity law is controlled by the grain size of sand. In this experiment, the actual sand in sea was used, so the similarity law was satisfied.

#### (1) Experimental equipment and method of sampling sand deposits

The experimental setup comprised a water tank (3 m<sup>3</sup>) on the upstream side of a 24 m water channel that was 0.5 m wide. The water channel consisted of a flat section, sand bed section, and slope section. Opening the gate of the tank generated a 0.1 m deep bore wave in the flat section. The slope section (slope: 1/40) comprised an impermeable surface roughened using sandpaper (#80). In the fixed bed condition, a sand bed section was fitted (slope: 1/20), the surface of which

was also impermeable and roughened using sandpaper (#80). Sand deposits transported on the slope by the bore wave were caught by a sand catcher. The sand catcher comprised a wooden frame with stainless steel plates dividing sections at equal intervals (0.2 × 0.2 m), as used by Harada et al.<sup>[9, 10]</sup>. Dropping the sand catcher onto the slope stopped the movement of the deposit and allowed collection of samples of the deposit of equal area. We employed two timings to catch the sand deposit: one when the wave reached the top of the run-up area and the other when the return flow had gone. The deployment position was set from the shoreline to the top of the run-up area. The sample of sand deposit collected from each section was measured for dry weight. For the case of mixed sand composition, sieving of grain sizes was conducted after drying.

#### (2) Method of measurement for fixed bed condition

Water level was measured using ultrasonic wave height meters, and the flow velocity was measured using both electromagnetic velocity meters and propeller velocity meters. For the fixed bed condition, we measured flow velocity and water level at many points because we needed to record detailed flow conditions.

The electromagnetic velocity meters measured at two points: 1.0 and 5.0 m (sand bed center) from the gate. The propeller velocity meters measured at eight points from the shoreline to 20 m from the shoreline at 2.0 m intervals. However, for the case of the reflection wall, measurements were acquired

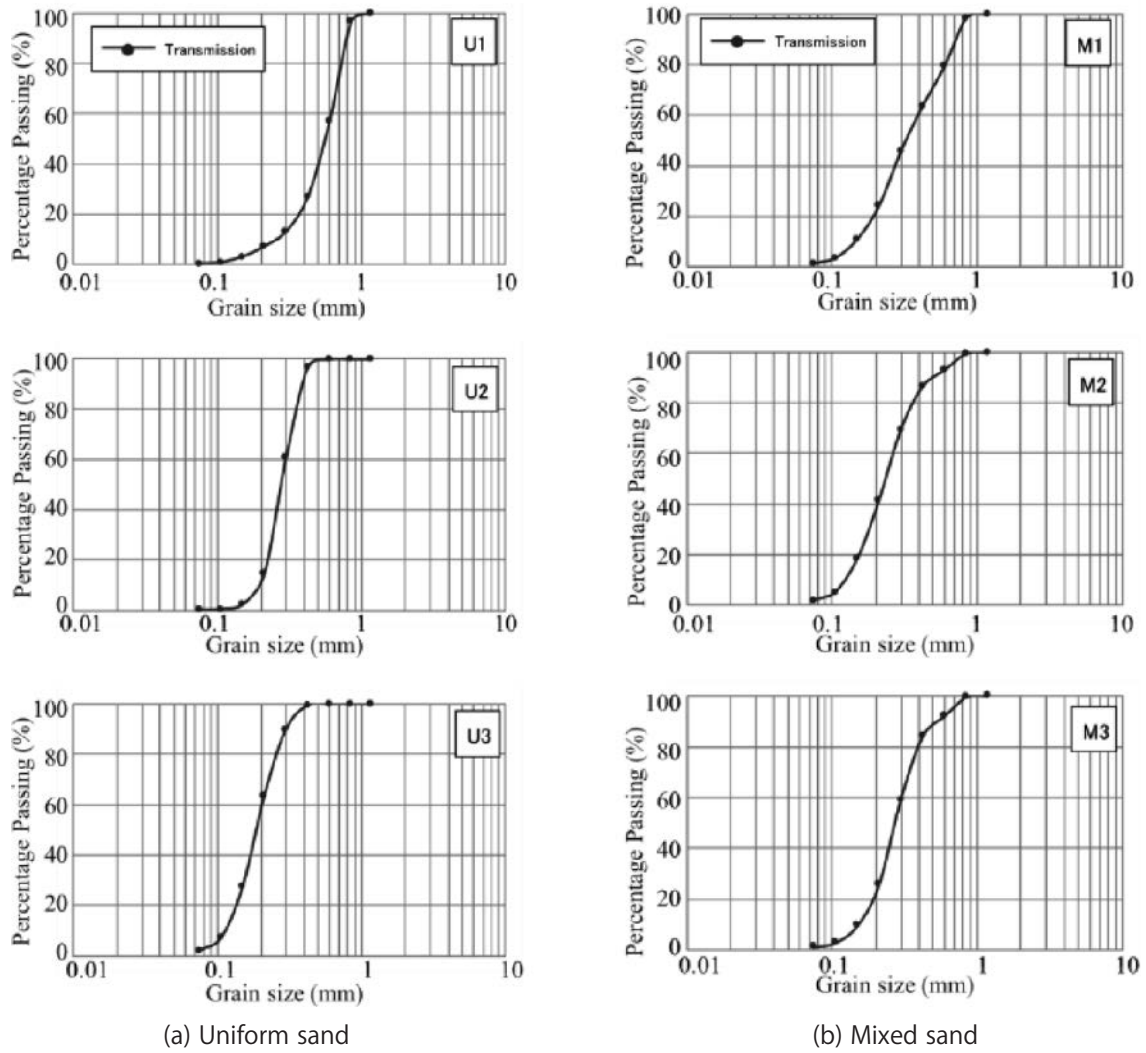


Figure 2. Grain size accumulation curves

at eight points (6.0, 7.1, 8.3, 8.9, 9.7, 11.1, 11.5, and 12.3 m) from the gate. Ultrasonic wave height meters were used to take measurements at the points of the velocity meter measurements. All measurement points were set central in the channel. The propeller velocity meters were set 1 cm above the bottom surface to measure the bottom velocity on the slope. For the movable bed condition, the velocity and water level were measured 1.0 m from the gate, as well as at the shoreline and the center of the sand bed. In

addition, turbidity meters were set at four points (6.0, 6.2, 7.0, and 7.8 m from the gate) on the slope near the shoreline. All case experiments were undertaken three times to confirm reproducibility. Furthermore, moving images were taken from the side of the sand bed, slope, and the top of the run-up area. These were used to measure the run-up distance from the shoreline and to confirm the behavior of the sand.

(3) Sand grain sizes and mixing ratios for

movable bed condition

The location and condition of the sand are shown in **Figure 1**. In this study, we investigated not only uniform sand, as in previous studies, but also mixed sand which has several grain sizes. The latter is more representative of reality.

The sand was set in the sand bed section as three types of uniform sand and three types of mixed sand. **Figure 2** shows their grain size accumulation curves after sieving. The median grain size of sand U1, U2, and U3 was 0.560, 0.279, and 0.189 mm, respectively. The mixing ratio is a ratio of mixed sand in mass (U1:U2:U3). The mixing ratio of M1, M2, and M3 were 4:4:2, 2:5:3, and 2:6:2, respectively. The sand bed section was completely submerged with initial water depth of 0.1 m. The sand in the sand bed section was allowed to set by settlement under submergence.

(4) Conditions of exerting forces

The sand conditions and exerting forces conditions of the experiments are listed in **Table 1**. The bore wave height was set to the water level difference  $H$  (25 cm) between the water tank and the initial water depth of the channel (0.1 m), which was also a height that did not overflow the slope. Two types of bore wave condition were investigated: return flow and nonreturn flow. For the case of nonreturn flow, it was considered that complete infiltration and flooding of low-lying land occurred. The case of return flow was set to consider the influence of the wave during run-up and return (i.e., case of a reflection wall). Furthermore, we not only investigated

Table 1. Grain sizes and experimental conditions (bore wave height: 25cm; number of waves: 1)

(a) Uniform sand

Sand condition ( $d_{50}$ mm)		Reflection wall	Return flow
U1	0.560	No	Yes
		Yes	No
U2	0.279	No	Yes
		Yes	No
U3	0.189	No	Yes
		Yes	No

(b) Mixed sand

Sand condition (mixed ratio; U1:U2:U3)		Reflection wall	Return flow
M1	4 : 4 : 2	No	No
M2	2 : 5 : 3	No	No
M3	2 : 6 : 2	No	No

run-up without structures but we also examined the sand deposits for cases restricted by topography and structures, for which the condition included a reflection wall installed on the slope. For details and results of the experiment, the reader is referred to Yamamoto et al.<sup>[11]</sup>.

2.2 Measurement Results and Considerations

All experiments in this study were conducted in triplicate for all cases to check reproducibility. Furthermore, the analysis of the measurement results used the average values of each set of three trials.

(1) Results of water level and velocity under fixed bed condition

The time series of water level and velocity at the bore wave height of 25 cm are shown in **Figure 3**. For the case of a run-up wave only (**Figure 3 (a) (b) upper panels**), both the

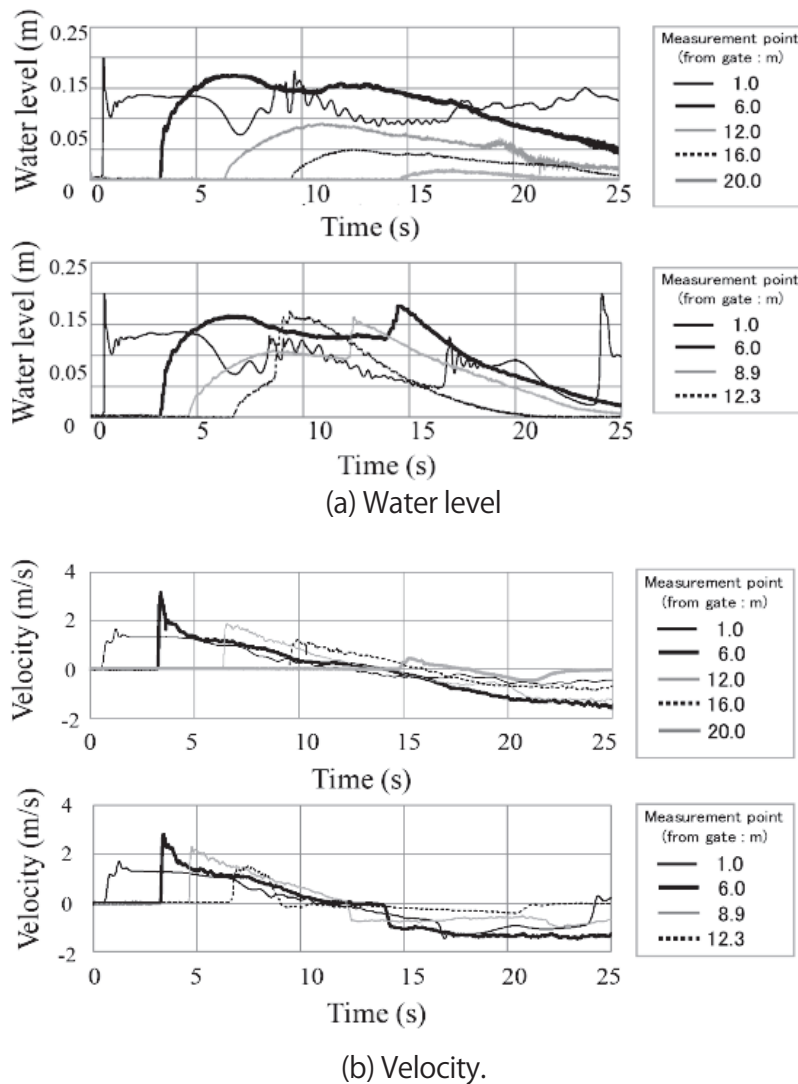


Figure 3. Water level and velocity at each measurement point in the fixed bed cases: (upper panels) nonreturn flow and (lower panels) return flow (i.e., reflection wall)

water level and the velocity show sharp increase during the time of the reaching bore wave as it traveled from near the gate to the shoreline. However, these changes are gradually less pronounced in the run-up area. For the case of the reflection wall (**Figure 3 (a) (b) lower panels**), the wave was reflected by the wall; thus, both the water level and the velocity exhibit a second sharp change in comparison with the reaching bore wave.

## (2) Comparison of the run-up distance between water and sand deposits

**Table 2** shows the run-up distances of water and sand from the shoreline. Here, DW is the run-up distance of water from the shoreline, DS is the run-up distance of sand from the shoreline, and DS/DW (%) is the distance reached by sand against the distance reached by water in terms of a percentage. DS was distinguished by the weight of sand exceeding

Table 2. Results of the run-up distance and DS/DW rate

	Hydraulic experiment			Calculation		
	DW	DS	DS/DW 【%】	DW	DS	DS/DW 【%】
U1	15.0	12.8	85.3	17.0	16.5	97.1
U2		12.6	84.0		16.9	99.4
U3		14.4	96.0		17.0	100
M1		13.8	92.0		17.0	100
M2		14.2	94.7		17.0	100
M3		13.6	90.7		17.0	100

0.01 g in the sand catcher.

Overall, when grain size became finer, the values of DS and DS/DW tended to increase in the uniform sand cases. This finding confirms the research of Abe et al.<sup>[3]</sup>. However, the run-up distances and DS/DW rate vary for the mixed sand cases, confirming the influence of grain size.

(3) Comparison of sand deposits in uniform sand cases

The total amounts of sand deposit in the uniform sand cases for a single wave (nonreturn flow) are shown in **Figure 4**. The vertical axis shows the amount of sand deposit and the horizontal axis shows the  $x/DW$  value (similarly in **Figures 5-8**).  $x$  is distance

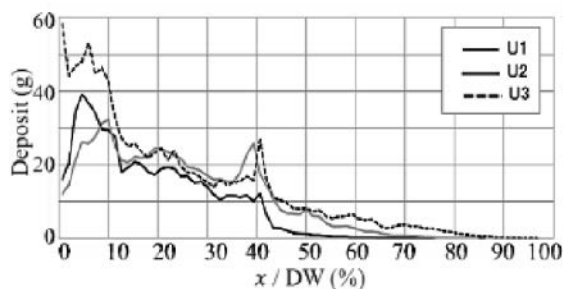


Figure 4. Comparison of the amount of sand deposit in uniform sand cases

of the sand from shoreline. The  $x/DW$  value made it possible to compare the outcomes of the different conditions.

Marked increases in the amounts of sand deposit near the shoreline and in the middle of the slope area are evident for all grain sizes. However, the amount of sand deposit remains largely unchanged between the area near the shoreline and the middle of the slope area. It is confirmed that the amount of sand deposit decreased toward the top of the run-up area with increasing grain size. In addition, the point of increase of sand deposit in the middle of the slope area was the same for all grain sizes, which suggests it is dependent on the exerting force. As shown in the middle of the slope area (12.0 m; gray thin line) in **Figure 3 (a)**, both the water level and the velocity decreased rapidly after 20 s. It is considered that a strong return flow was beginning to occur at the time of deployment of the sand catcher. Similarly, the increase in the shoreline area is considered caused by the difference in flow condition during deployment of the sand catcher. These factors are likely dependent on this specific experiment.

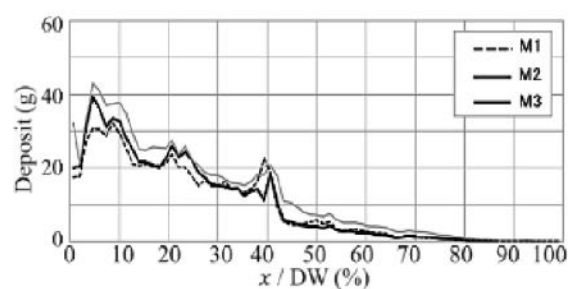
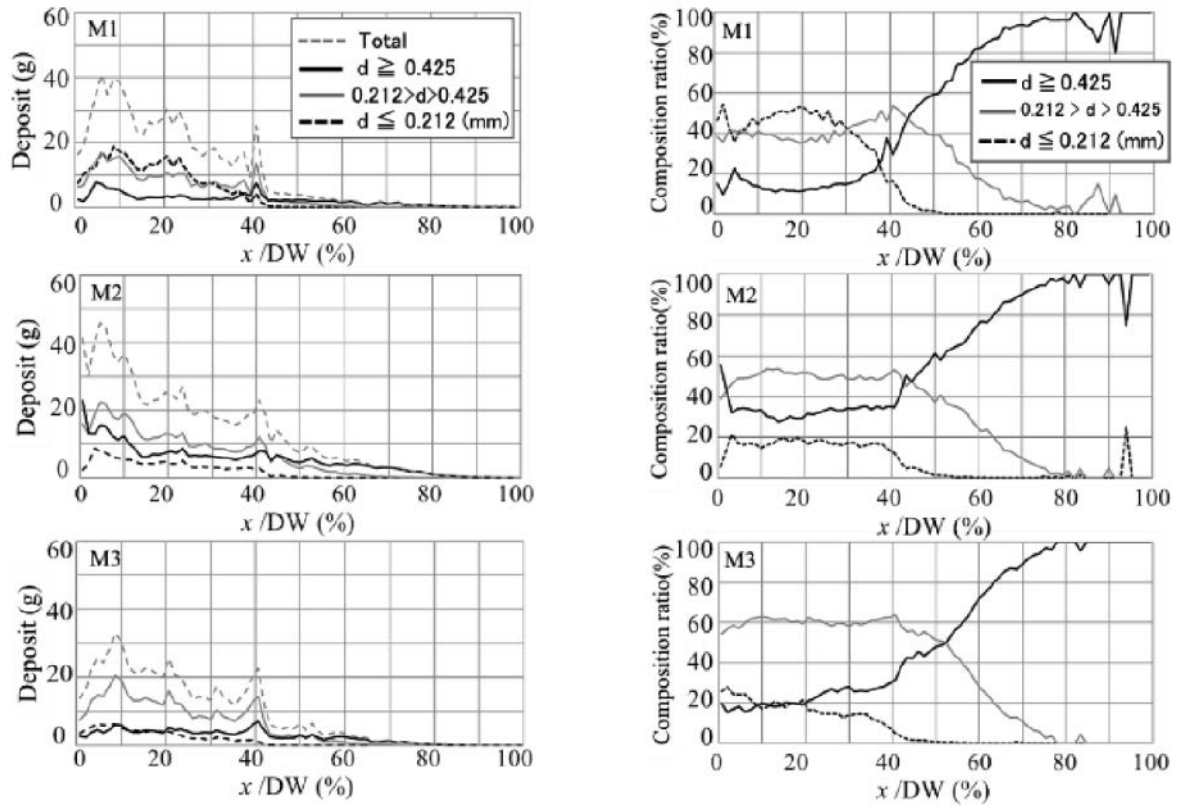


Figure 5. Comparison of the amount of sand deposit in mixed sand cases



(a) Comparison of each grain size and total sand deposit

(b) Composition ratio of each grain size

Figure 6. Comparison of grain size after sieving to total sand deposit, and composition ratio of each grain size

(4) Comparison of sand deposits in mixed sand cases

The total amounts of sand deposit in the mixed sand cases for a single wave (nonreturn flow) are shown in **Figure 5**. Although the mixing ratios differed, the total amounts of sand deposit showed little variation between three cases. Moreover, the patterns of increase/decrease of sand deposit were found similar to the cases of uniform sand. Thus, it is considered that the sand deposit of mixed sand was affected more by the exerting force than by the mixing ratio.

Comparison between the amount of sand deposit for each grain size and the total

amount of sand deposit (gray dotted line) is shown in **Figure 6 (a)**. **Figure 6 (b)** shows the composition ratio of each grain size to the amount of sand deposit. As shown in **Figure 5**, there was almost no difference in the total amount of sand deposit for each case. However, it is revealed that the amount of sand deposit and the grain size of the sand composition differed greatly at each measurement point. As shown in **Figure 6 (b)**, the coincidence of the composition and mixing ratios was very high at the  $x/DW$  value of 40% from the shoreline. In addition, it is confirmed that the amount of sand deposit decreased toward the top of the run-up area

with increasing grain size. Furthermore, it is revealed that the amount of sand deposit of mixed sand composition has high correlation with the amount of sand deposit of medium grain size by sieving. This result confirms the similar trends found in the case of Yamamoto et al.<sup>[11]</sup> and in the case of a different slope and exerting force of Harada et al.<sup>[10]</sup>.

#### (5) Comparison of sand deposits in reflection wall installation

In experiments by Harada et al.<sup>[9]</sup>, sand deposit on the slope area could be confirmed even under the condition of a return flow. The reason for this was considered the difference in the bore wave period between the experiments of this study and Harada et al.<sup>[9]</sup>. The bore wave period in this study was longer; therefore, it is considered that the influence of the return flow was dominant. Furthermore, the actual tsunami run-up was not necessarily the same as the flow condition of the wave with run-up only (i.e., nonreturn flow) and the wave with return flow in this study. It is considered that many cases were affected by topography and structures. In this study, we set a reflection wall in the slope area and we investigated the influence of topography and structures. The bore wave was forcibly reflected on its way to the run-up area by the reflection wall.

The amount of sand deposit in a single wave case (i.e., with return flow and reflection wall) is shown in **Figure 7**. For the case with a reflection wall, it is confirmed that sand deposit was generated on the slope in contrast to the condition of a return flow without a

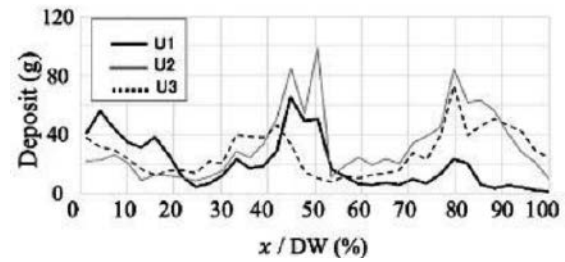


Figure 7. Comparison of the amount of sand deposit with reflection wall for uniform sand cases

reflection wall. As shown in **Figure 3 (b)**, the reflection wall caused a sudden increase of the water level and a decrease of the velocity. Therefore, it is considered that the Shields number decreased and that a large amount of sand was deposited under this flow condition. Furthermore, the amount of sand deposit on the slope repeatedly increased and decreased. In particular, increases of the sand deposit are confirmed near the shoreline, in the middle of the slope, and near the reflection wall. There are several possible causes of such phenomena. First, the turbulence of the flow generated by the reflection wall is very large compared with the case without a reflection wall, which could result in increased deposition of sand on the slope. Second, it could be considered that some sand deposit was not transported because the return flow was not sufficiently developed.

### 3. VALIDATION OF SEDIMENT TRANSPORT MODEL

#### 3.1 Sediment Transport Model

The 2000 model is a sediment transport model that focuses on the differences in the forms of transportation of sand. It defines sediment transportation under special flow

conditions, e.g., a tsunami, by separating the suspended load and the bed load. In this model, the amount of sand transport is treated as a function of the bed load transport rate and the sand exchange rate. The governing equations, shown below, were proposed based on the laws of mass conservation and momentum conservation:

$$\frac{\partial Z_B}{\partial t} + \frac{1}{1-\lambda} \left( \frac{\partial q_{Bx}}{\partial x} + \frac{\partial q_{By}}{\partial y} + w_{ex} \right) = 0, \quad (1)$$

$$\frac{\partial \bar{C}_s M}{\partial x} + \frac{\partial \bar{C}_s N}{\partial y} - w_{ex} + \frac{\partial \bar{C}_s h_s}{\partial t} = 0, \quad (2)$$

$$q_B = a \sqrt{sgd^3} \tau_*^{3/2}, \quad (3)$$

$$w_{ex} = b \tau_*^2 - \frac{w_0 \bar{C}_s}{\sqrt{sgd}}, \quad (4)$$

where  $Z_B$  is the height of the bottom from the reference point,  $\lambda$  is the porosity of the sand,  $q_B$  is the bed load transport rate,  $w_{ex}$  is the sand exchange rate,  $\bar{C}_s$  is the average concentration of the suspended loads,  $M$  and  $N$  are the discharge of the  $x$  and  $y$  axis, respectively,  $h_s$  is the thickness of the suspended load,  $w_0$  is the settling velocity,  $\tau_*$  is the Shields number,  $s$  is the specific gravity of sand in water,  $g$  is the acceleration of gravity,  $d$  is the grain size. and  $a$  and  $b$  are coefficients, determined as 21 and 0.012, respectively, by hydraulic experiment.

Equations (1)-(4) represent the continuity equation of the bed load, continuity equation of the suspended load, equation of motion of the bed load transport rate, and equation of motion of the sand exchange rate, respectively. In addition,  $\tau_*$ , calculated using the friction velocity obtained by the flow

velocity, is defined as follows:

$$\tau_* = \frac{u_*^2}{sgd}, \quad (5)$$

where  $u_*$  is the friction velocity.

The 2000 model assumes sediment transport with a single grain size. Therefore, the same values of coefficients  $a$  (Eq. (3)) and  $b$  (Eq. (4)) are adopted in this model for all grain sizes. To reflect real situations, it is necessary to assume sediment transport of mixed sand composition. Conversely, Takahashi et al.<sup>[6]</sup> focused on the coefficient of the equation of motion of sediment transport, for which the coefficients for different grain sizes were defined as follows by hydraulic experiment:

$$a = \begin{cases} 5.6 & (d=0.166mm) \\ 4.0 & (d=0.267mm) \\ 2.6 & (d=0.394mm) \end{cases}$$

and

$$b = \begin{cases} 7.0 \times 10^{-5} & (d=0.166mm) \\ 4.4 \times 10^{-5} & (d=0.267mm) \\ 1.6 \times 10^{-5} & (d=0.394mm) \end{cases}$$

The governing equations of flow use nonlinear shallow-water equations in both models. The following shows the continuity equation (**Eq. 6**) and the equations of motion (**Eqs. 7 and 8**):

$$\frac{\partial \eta}{\partial t} + \frac{\partial M}{\partial x} + \frac{\partial N}{\partial y} = 0, \quad (6)$$

$$\frac{\partial M}{\partial t} + \frac{\partial}{\partial x} \left( \frac{M^2}{D} \right) + \frac{\partial}{\partial y} \left( \frac{MN}{D} \right) + gD \frac{\partial \eta}{\partial x} + \frac{gn^2}{D^{7/3}} M \sqrt{M^2 + N^2} = 0, \quad (7)$$

$$\frac{\partial N}{\partial t} + \frac{\partial}{\partial x} \left( \frac{MN}{D} \right) + \frac{\partial}{\partial y} \left( \frac{N^2}{D} \right) + gD \frac{\partial \eta}{\partial y} + \frac{gn^2}{D^{7/3}} N \sqrt{M^2 + N^2} = 0, \quad (8)$$

where  $\eta$  is water level,  $D$  is total depth of water (i.e.,  $\eta+h$ ), and  $h$  is still water depth. The computation scheme uses the Leap-frog scheme with a staggered grid in both models.

### 3.2 Conditions in Reproduction Calculation

**Table 3** shows the common calculation conditions used in the reproductions of both models of Takahashi et al.<sup>[4, 6]</sup>. The boundary

condition used water level data at 1.0 m from the gate. The actual simulation time of run-up without a return flow stops the calculation on reaching the top of the run-up area. Conversely, the actual simulation time of run-up with a return flow (i.e., the case with a reflection wall) stops the calculation when the return flow reaches the shoreline. **Table 4** shows the parameters that were changed in each model. Coefficients  $a$  and  $b$  were set by interpolation of the coefficients used in the model of Takahashi et al.<sup>[6]</sup>. The settling velocity was set based on the Rubey experimental formula. The Manning's roughness coefficient was set using the Manning's roughness coefficient conversion formula. The critical friction velocity was set based on the critical friction velocity

Table 3. General conditions of calculation

Calculation condition	Fixed bed	Movable bed (without reflection wall)	Movable bed (with reflection wall)
Number of grids	52 × 2300		52 × 1300
Grid interval (m)	0.01		
Time interval (s)	0.001		
Calculation steps	40000	25000	32000
Actual simulation time (s)	40	25	32

Table 4. Conditions of sediment transport in each model

	Takahashi et al. (2000)	Takahashi et al. (2011)		
		U1	U2	U3
Grain size (mm)	—	0.560	0.279	0.189
Coefficient $a$	21.0	5.19	3.83	1.49
Coefficient $b$	0.012	$0.57 \times 10^{-5}$	$3.59 \times 10^{-5}$	$6.46 \times 10^{-5}$
Settling velocity (m/s)	0.03	0.0677	0.0374	0.0234
Manning's roughness coefficient	0.015 (sand bed and slope section) 0.0 (flat section)	0.0131	0.0118	0.0112
Critical shear velocity (m/s)	0.01314	0.0213	0.0150	0.0116

conversion formula.

### 3.3 Comparison of Measurement Results and Calculation Results

#### (1) Reproduction of water level and velocity

The measurement (gray line) and calculation (black line) results of the water level at five observation points (i.e., 1.0, 5.0, 6.0, 10.0, and 14.0 m from the gate) are shown in **Figure 8**. The measurement (gray line) and calculation (black line) results of velocity at the same five observation points are shown in **Figure 9**. It is confirmed that the measurement and calculation results were in reasonable agreement with regard to water level, but that there was slight difference in

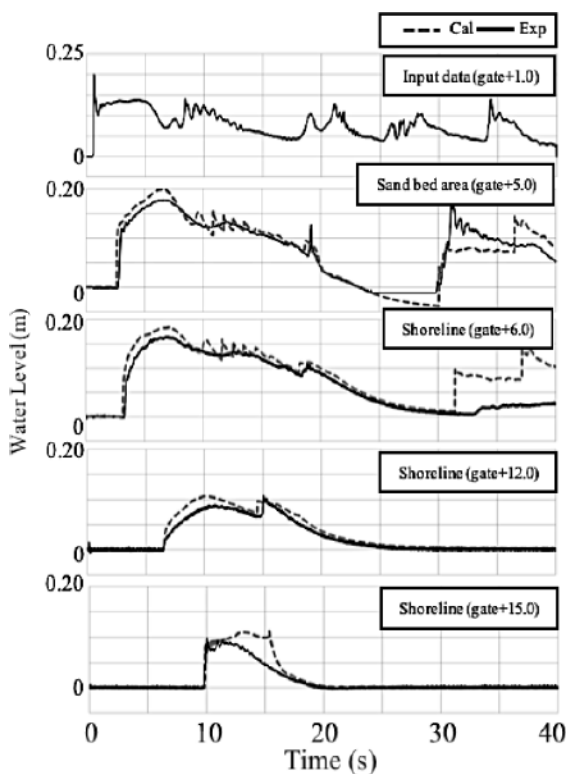


Figure 8. Comparison of water level at each measurement point with calculation results

the reaching time of velocity on the slope area. Nevertheless, it is confirmed that the displacement and phase were in reasonable agreement.

#### (2) Reproduction of run-up distance for water and sand

**Table 2** presents the calculation results of the run-up distance. It is confirmed that both the run-up distance and the DS/DW rate were highest for the finer grain size, similar to the results of the experiment described in 2.2.2. However, it became clear that both the run-up distance and the DS/DW rate tended to be overestimated.

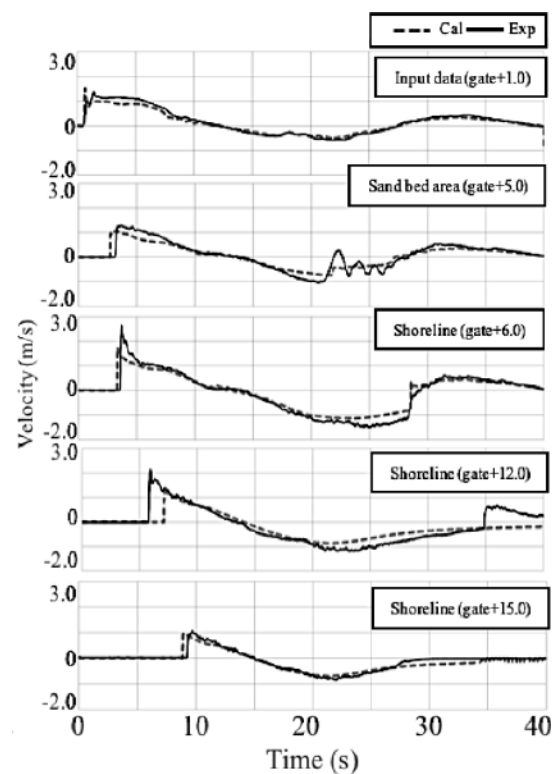


Figure 9. Comparison of velocity at each measurement point with calculation results

### 3.4 Comparison of Reproduction in Present Model

The amount of sand deposit in the experiment (gray line) and the calculation results for each grain size U1-U3 are shown in **Figure 10**. Comparison of the total amount of sand transport and the rate of agreement confirm that the 2011 model (black solid line) outperformed the 2000 model (black dotted line). However, the 2011 model had lower reproducibility in the coarse sand case (U1). In addition, the peak of the sand deposit tended to be biased toward the front of the run-up area. Nevertheless, it is confirmed that this was improved slightly in the 2011 model. Interestingly, it was revealed that the run-up distance of the sand deposit was

overestimated around the front of the run-up area in both models. Furthermore, the amount of sand deposit was underestimated near the shoreline. The sand bed section near the shoreline in the experiment experienced considerable scouring by the return flow. Therefore, it is conceivable that turbulence became large near the shoreline. It is confirmed that the near-shoreline area was influenced considerably by flow conditions, and that these conditions varied between the experiment and the calculations. Consequently, this study neglected further comparison of the near-shoreline area.

The amounts of sand deposit (gray line) in the mixed sand experiment cases and the calculation results are shown in **Figure 11**. The

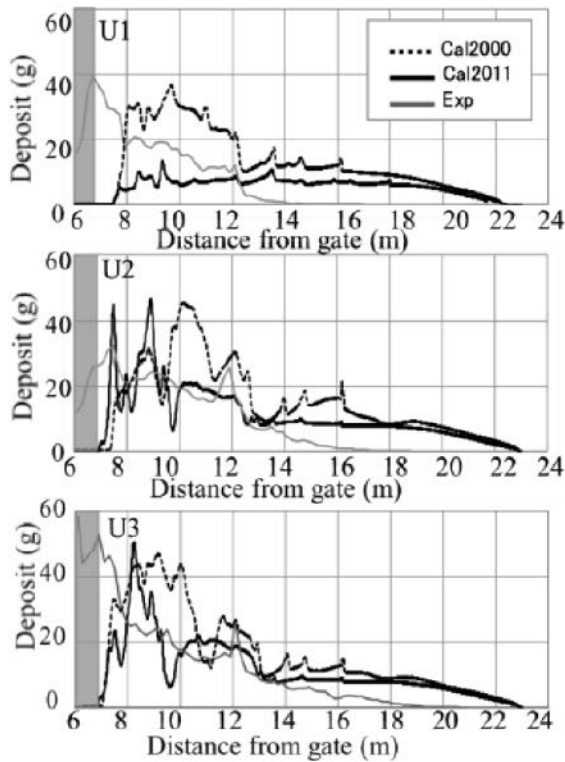


Figure 10. Comparison of sand deposits and calculation results for uniform sand cases

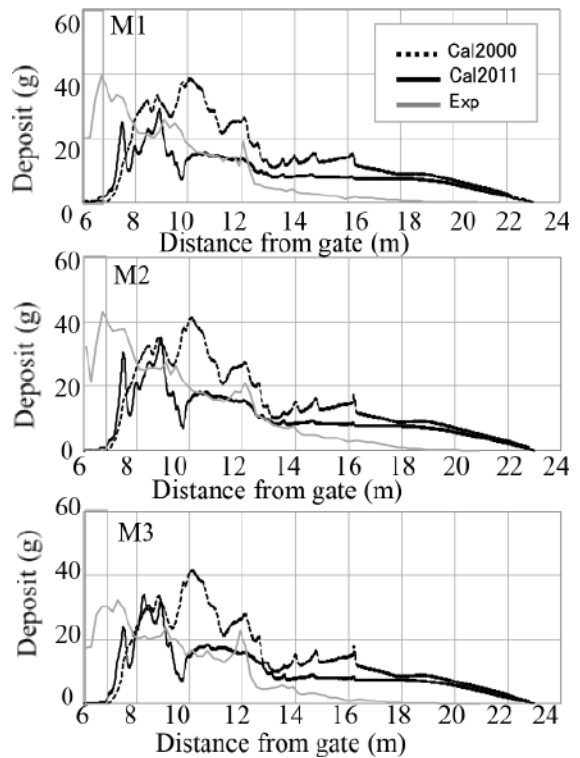


Figure 11. Comparison of sand deposits and calculation results for mixed sand cases

2011 model (black solid line) is confirmed to have better reproducibility than the 2000 model with regard to the amount of sand deposit and it produced a high coincidence ratio for all mixing ratios. However, it is confirmed that the amount of sand deposit was biased toward the top of the run-up area and that the distance of the sand deposit was overestimated around the front of the run-up area, as in the case of uniform sand.

The amounts of sand deposit (gray line) in the experiment and the calculation results for the case of a reflection wall are shown in **Figure 12**. The 2011 model (black solid line) was found to have reasonable reproducibility with regard to the amount of sand deposit and it produced a high coincidence ratio. Furthermore, the reproducibilities of the peak of the coincidence ratio and of the amount of sand deposit were improved for the case of a reflection wall. A return flow was not considered for cases without a reflection wall.

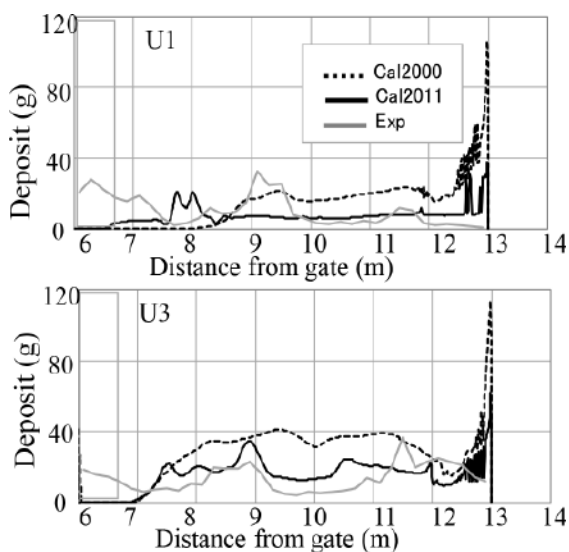


Figure 12. Comparison of sand deposits and calculation results for cases with a reflection wall

However, it was considered for cases with a reflection wall, which confirmed reproducibility was high in the present model as long as the conditions included a return flow.

#### 4. PROBLEMS IN THE PRESENT MODEL

The results of this study confirm that reproducibility was high in the 2011 model; however, certain problems with the model were revealed. First, it became clear that the amount of sand deposit was biased toward the top of the run-up area. Furthermore, it was apparent that the distance of sand transportation was overestimated at the top of run-up area. Reproducibility was found to decline with grain size (U1) in the 2011 model. As mentioned in section 3.4, it is confirmed that reproducibility was high for the case of a reflection wall with a return flow. In the present model, it seems there are problems regarding the form of transport of sand in cases without a return flow. Therefore, with consideration of the process of sand transport, we propose certain measures to improve reproducibility. Several factors have substantial influence on sediment transport, e.g., bed load and suspended load concentrations, the Shields number, settling velocity, and the coefficients (bed load transport rate and sand exchange rate) in the equation of motion of sand transport. We have already considered the coefficients and settling velocity in the present model. Therefore, it is important to focus on the concentration at the boundary between the bed load and the suspended load. In the present model, the concentration at the boundary was calculated

using the average concentration. Even with an average concentration, reproducibility can be ensured in the present model under the conditions of equilibrium flow. However, under the conditions of nonequilibrium flow, as in a tsunami, the flow rate changes rapidly. Therefore, it is highly possible that the reproducibility was underestimated. We considered using the concentration at the boundary between the bed load and the suspended load at each point and time step. It is considered that improved representation of the concentration between the bed load and the suspended load, using the formula of Itakura and Kishi<sup>[14]</sup>, will help overcome this problem in the present model.

Moreover, the friction velocity of the present model used Manning's rule; however, this is not reproducible under nonequilibrium flow conditions. Therefore, we considered the use of the log-wake rule, which can be applied under the conditions of high pressure found in a tsunami, for further improvement of the model.

## 5. CONCLUSION

In this study, hydraulic experiments were conducted to clarify the formation mechanism of tsunami deposits using a two-dimensional water channel. The experimental conditions changed both the grain size of the sand and the reflection wave. For both uniform and mixed sand cases, it is confirmed that the amount of sand deposit decreased toward the top of the run-up area. For the mixed sand cases, the coincidence of the composition and mixing ratios was very high at the  $x/DW$

value of 40% from the shoreline. Furthermore, it was revealed that the medium grain size had the highest correlation with the total amount of sand deposit. For the case of the reflection wall, it is confirmed that the sand deposit was not removed by the return flow.

In this study, we reproduced the models of Yamamoto et al.<sup>[11]</sup> and Takahashi et al.<sup>[4, 6]</sup>, elucidated the problems, and suggested improvements for the present model. Consequently, it is confirmed that the 2011 model showed greater agreement than the 2000 model with experimental data, although the 2011 model had decreased reproducibility for coarse sand (U1). In addition, the peak of the sand deposit tended to be biased toward the front of the run-up side. However, it was revealed that the run-up distance of the sand deposit was overestimated around the front of the run-up area in both models. Finally, it is confirmed that reproducibility is high in the present model as long as the conditions include a return flow. Based on the results of this study, to overcome some of the problems inherent in the present model, we proposed using the concentration at the boundary between the bed load and the suspended load at each point and time step.

## Acknowledgments

This study was supported by JSPS KAKENHI Grant Number 17H02060. In addition, part of hydraulic experiment was carried out in the commissioned project of the Secretariat of Nuclear Regulation Authority.

## References

- [1] Futoshi Nanayama, Akito Makino, Kenji Satake, Ryuta Furukawa, Yoshiharu Yokoyama and

- Mitsuru Nakagawa (2001). *Twenty tsunami event deposits in the past 9000 years along the Kuril subduction zone identified in Lake Harutori-ko, Kushiro City, eastern Hokkaido, Japan*. Annual Report on Active Fault and Paleoearthquake Researches. No.1, p. 233-249.
- [2] Osamu Fujiwara, Takanobu Kamataki, Jun-ichi Ueda, Kouhei Abe and Tsuyoshi Haraguchi (2009). *Early Holocene coseismic uplift and tsunami deposits recoded in a drowned valley depositon the SE coast of the Boso Peninsula, central Japan*. The Quaternary Recerch. Vol.48 (1), pp1-10.
- [3] Tomoya Abe, Kazuhisa Goto, Daisuke Sugawara (2012). *Relationship between the maximum extent of tsunami sand and the inundation limit of the 2011 Tohoku-oki tsunami on the Sendai Plain, Japan*. Sedimentary Geology. 282, pp.142-150.
- [4] Tomoyuki Takahashi, Nobuo Shuto, Fumihiko Imamura, and Daisuke Asai (2000). *Modeling sediment transport due to tsunamis with exchange rate between bedload layer and suspended load layer*. Proc. of the Int. Conf. Coastal Engineering. pp. 1508-1519.
- [5] Yu Morishita, and Tomoyuki Takahashi (2014). *Accuracy improvement of movable bed model for tsunamis by applying for Kesennuma bay when the 2011 Tohoku tsunami arrived*. J. of JSCE, B2 (Coastal Engineering). Vol. 70, pp. 491-495.
- [6] Tomoyuki Takahashi, Takehiro Kurokawa, Masataka Fujita, and Hiroaki Shimada (2011). *Hydraulic experiment on sediment transport due to tsunamis with various sand grain size*. J. of JSCE, B2 (Coastal Engineering). Vol. 67, pp. 231-235.
- [7] Bruce Jaffe, Kazuhisa Goto, Daisuke Sugawara, Guy Gelfenbaum, and SeanPaul La Selle (2016). *Uncertainty in Tsunami Sediment Transport Modeling*. Journal of Disaster Research. Vol.11, No.4, pp.647-661.
- [8] Shiro Hasegawa, Tomoyuki Takahashi, Yoshiyuki Uehata (2001). *Hydraulic Experiment on Sediment due to Tsunami Run-up*. Proceedings of Coastal Engineering, JSCE. Vol.48, pp.311-315.
- [9] Kenji Harada, Kentaro Imai, Tran The Anh, and Yoshifumi Fujiki (2011). *Hydraulic experiment on sand deposit by tsunami run-up with land slope*. J. of JSCE, B2 (Coastal Engineering). Vol. 67, pp. 251-255.
- [10] Kenji Harada, Tomoyuki Takahashi, and Kazuya Nojima (2017). *Hydraulic experiment for distribution of sand deposit formed on slope by tsunami*. J. of JSCE, A1 (Structural Engineering & Earthquake Engineering). Vol. 73, pp. 634-641.
- [11] Ako Yamamoto, Tomoyuki Takahashi, Kenji Harada, Masaaki Sakuraba, and Kazuya Nojima (2017). *Hydraulic experiment on tsunami deposits formation related with sand grain and bore wave*. J. of JSCE, B2 (Coastal Engineering). Vol. 73, pp. 367-372.
- [12] Tomoyuki Takahashi, Fumihiko Imamura, Nobuo Syuto (1991). *Tsunami Induced Currents and Change of Sea Bottom Configuration - Kesennuma Bay in Case of the 1960 Chilean Tsunami -*. Proceedings of Coastal Engineering, JSCE, Vol. 38, pp. 161-165.
- [13] Shiro Hasegawa, Tomoyuki Takahashi, Yoshiyuki Uehata (2001). *Hydraulic experiment on sediment due to tsunami run-up*. J. of JSCE, B2 (Coastal Engineering). Vol. 48, pp. 311-315.
- [14] Tadaoki Itakura and Tsutomu Kishi (1980). *Open channel flow with suspended sediments*. J. of Hyd. Dyv., ASCE. Vol. 106, HY8, pp.1325-1343.

(原稿受付日：2018年9月28日)

(掲載決定日：2018年11月29日)

